

Numerical Solution of Nonlinear Cross Diffusion Problems

Günter Bärwolff(✉) and Julia Baumbach

Institute of Mathematics, Technische Universität Berlin, Straße des 17. Juni 136, 10623 Berlin, Germany
baerwolf@math.tu-berlin.de

Abstract. This paper considered cross-diffusion equations. With those equations the concentration development in a certain region during an interesting time-interval can be described.

Cross-diffusion means the diffusion of some species which influence each other. The population dynamics of different species is a famous example of cross-diffusion.

The implicit time-integration of such parabolic equations leads to nonlinear equation systems which requires a huge computational amount.

To avoid this amount we discuss a linear scheme proposed by Murakawa [2] and investigate his properties.

Keywords: Cross diffusion problems, Linear time integration scheme · Finite volume method

1 Introduction

This paper deals with the so called cross-diffusion equations. These are nonlinear parabolic partial differential equations and there components influence each other. This means that every component of the solution we are looking for was influencing the other ones and vice versa. Compared to classic diffusion equations it is necessary to solve nonlinear equation system in the case of implicit time integration schemes (Euler backward). But we will discuss special linear schemes which are easy to implement. These schemes are very sensitive but they are a good alternative to the huge amount in the case of the solution nonlinear equation system with a certain kind Newtons method.

1.1 Some Necessary Terms and Definitions

In this paper Ω describes a 1d or 2d bounded region with a smooth boundary $\partial\Omega$. On this region we investigate the concentration during the time in the interval $[0, T]$ where $T > 0$. Our cross diffusion system lives on the space-time cylinder $Q = \Omega \times (0, T]$. $M \in \mathbb{N}$ is the number of considered species which influence each other. For vector valued functions (for example $z : \mathbb{R}^M \to R^M$) we denote the i-th component by z_i $(i = 1, \ldots, m)$. With Z^n we denote the approximation of a function z at the n-th time step. With a bold sub-index, for instance z_0 or Z_0 we denote the given initial conditions.

© Springer Nature Switzerland AG 2019
S. Misra et al. (Eds.): ICCSA 2019, LNCS 11619, pp. 13–24, 2019.
https://doi.org/10.1007/978-3-030-24289-3_2

1.2 The Cross-Diffusion Equations

With the above discussed preparations we will now formulate the cross-diffusion equations. We are looking for a function $z = (z_1, \ldots, z_M) : \bar{\Omega} \times (0, T] \to \mathbb{R}^M$, $M \in \mathbb{N}$ with

$$\begin{aligned} \frac{\partial \mathbf{z}}{\partial t} &= \Delta\beta(\mathbf{z}) + f(\mathbf{z}) \quad \text{in } Q \\ \beta(z) &= \mathbf{0} \quad \text{on } \partial\Omega \times (0, T], \\ \mathbf{z}(\cdot, 0) &= \mathbf{z_0} \quad \text{in } \Omega. \end{aligned} \tag{1}$$

The functions $\beta = (\beta_1, \ldots, \beta_M)$ and $f = (f_1, \ldots, f_M)$ are defined as functions

$$\beta, f : \mathbb{R}^M \to \mathbb{R}^M.$$

$\mathbf{z_0} = (z_{01}, \ldots, z_{0M}) : \Omega \to \mathbb{R}^M$ are the given initial conditions. To illustrate the nonlinearity of the cross-diffusion problems we write down an example of Shigesada, Kawasaki and Teramoto [1] for two different components

$$\begin{aligned} \frac{\partial z_1}{\partial t} &= \Delta[(a_1 + b_1 z_1 + c_1 z_2) z_1] + (g_{10} - g_{11} z_1 - g_{12} z_2) z_1, \\ \frac{\partial z_2}{\partial t} &= \Delta[(a_2 + b_2 z_2 + c_2 z_1) z_2] + (g_{20} - g_{21} z_1 - g_{12} z_2) z_2, \end{aligned} \tag{2}$$

This model describes the competition of two different populations which influence each other. a_i, b_i, c_i and g_{ij} are non-negative constants ($i = 1, 2$, $j = 0, 1, 2$). z_1, z_2 describe the population density of the species. g_{i0} is the growth-rate of the i-th species while g_{ii} stands for an intra-specific concurrence value and g_{ij}, $i \neq j$ stands for the inter-specific concurrence value.

The obvious time integration scheme, for example used by Chen and Jüngel [4], is

$$\begin{aligned} \frac{\mathbf{Z}^n - \mathbf{Z}^{n-1}}{\tau} &= \Delta\beta(\mathbf{Z}^n) + f(\mathbf{Z}^n) \quad \text{in } \Omega, \\ \beta(\mathbf{Z}^n) &= \mathbf{0} \quad \text{on } \partial\Omega, \end{aligned} \tag{3}$$

where τ is the used time-step. But the time-discretisation (3) means the solution of a nonlinear equations system

$$\mathbf{Z}^n - \tau\Delta\beta(\mathbf{Z}^n) - \tau f(\mathbf{Z}^n) = \mathbf{Z}^{n-1}$$

in every time-step.

The scheme (3) is applicable but there some disadvantages like very huge non-symmetric matrices because of the necessary spatial discretisation which will discussed a bit later. To overcome the named problems Murakawa [2] developed an approximative time integration scheme for the solution of cross-diffusion problems of type (1). This algorithm should be discussed in the next sections.

2 Murakawas Method

We consider the discretisation of the time interval $[0, T]$ with the time-step $\tau = T/N_T$, $N_T \in \mathbb{N}$. Instead of a straight-forward Euler-backward method Murakawa proposed the following linear scheme

$$\begin{aligned} \mathbf{U}^n - \frac{\tau}{\mu}\Delta\mathbf{U}^n &= \beta(\mathbf{Z}^{n-1}) + \frac{\tau}{\mu}f(\mathbf{Z}^{n-1}) \quad \text{in } \Omega, \\ \mathbf{U}^n &= \mathbf{0} \quad \text{on } \partial\Omega, \\ \mathbf{Z}^n &:= \mathbf{Z}^{n-1} + \mu(\mathbf{U}^n - \beta(\mathbf{Z}^{n-1})) \quad \text{in } \Omega. \end{aligned} \tag{4}$$

μ is a free parameter which can be used to optimise the method. $\mathbf{U}$ is an approximation of $\beta(\mathbf{Z})$. $\mathbf{Z}^n$ is an approximation of $z(\cdot, n\tau)$.

There are also other boundary conditions than the second line of (4) possible, for example homogeneous or inhomogeneous Neumann boundary conditions. The advantage of the scheme (4) consists in the very friendly equation for the solution of $\mathbf{U}^n$ which is elliptic and leads after the spatial discretisation to a linear equation system with a positiv-definite coefficient matrix.

3 Some Mathematical Properties of the Scheme (4)

With the choice of appropriate Hilbert-spaces it is possible to formulate (4) in a weak form. Murakawa proved the existence of weak solutions $\mathbf{U}$ and $\mathbf{Z}$ and if we interpret these solutions as piece-wise constant interpolations during the time the following proposition holds. The main assumptions on the initial value and the functions β and f are

(1) β is Lipschitz-continuous with $\beta(\mathbf{0}) = \mathbf{0}$
(2) f is Lipschitz-continuous
(3) There is a constant $a > 0$ with

$$\sum_{i=1}^{M}((\beta_i(\xi) - \beta_i(\eta))(\xi_i - \eta_i) \geq a|\xi - \eta|^2$$

for a.e. $\xi, \eta \in \mathbb{R}^M$
(4) It should be $\mathbf{z}_0 \in L^2(\Omega)^M$

With (1) to (4) the main assumptions of the propositions of convergence and stability of the discussed methods are valid. The conditions (1) and (3) guarantee the parabolicity of the above noted cross-diffusion system. In the following should only mentioned some basic results of the method.

Theorem 1. *We have for the weak solution* $\mathbf{z} \in L^2(\Omega)^M$ *the global error*

$$\begin{aligned} E := \; & ||\beta(\mathbf{z}) - \mathbf{U}||_{L^2(\Omega)^M} + ||\int_0^t (\beta(\mathbf{z}) - \mathbf{U})dt||_{L^\infty(0,T;H^{-1}(\Omega))^M} \\ & + ||\mathbf{z} - \mathbf{Z}||_{L^\infty(0,T;H^{-1}(\Omega))^M} \end{aligned}$$

and the estimation

$$\mathbf{z} \in L^2(\Omega)^M \longrightarrow E + ||\mathbf{z} - \mathbf{Z}||_{L^2(Q)^M} = O(\sqrt{\tau})$$
$$\mathbf{z} \in L^2(\Omega)^M \longrightarrow E + ||\mathbf{z} - \mathbf{Z}||_{L^2(Q)^M} = O(\tau)$$

This means convergence and stability.

To prove this theorem one need several lemmata and theorems of the theory of Hilbert- and Sobolev-spaces (compactness and imbedding theorems) which can found in the papers of Murakawa [2,3].

To get an idee of finding a good choice of the parameter μ we consider the equivalent formulations of (1) and (4)

$$\frac{1}{\beta'(\mathbf{z})}\frac{\partial \beta(\mathbf{z})}{\partial t} = \Delta\beta(\mathbf{z}) + f(\mathbf{z})$$
$$\frac{\partial \mathbf{z}}{\partial t} = \frac{1}{\beta'(\mathbf{z})}\frac{\partial \beta(\mathbf{z})}{\partial t}$$

and

$$\mu\frac{\mathbf{U}^n - \beta(\mathbf{Z}^{n-1})}{\tau} = \Delta\mathbf{U}^n + f(\mathbf{Z}^{n-1}),$$
$$\frac{\mathbf{Z}^n - \mathbf{Z}^{n-1}}{\tau} = \mu\frac{\mathbf{U}^n - \beta(\mathbf{Z}^{n-1})}{\tau}$$

If we compare the continuous and the time-discrete system we find that

$$\mu \approx \frac{1}{\beta'(\mathbf{z})}$$

is a good choice. But the choice of μ can and should also be supported by numerical experiments.

4 Discretisation of (3) and (4) in Space

We use a finite-volume method for the spatial discretisation. This means we consider the balance of the fluxes on the boundary of finite volumes, in a number K 1d finite intervals and in 2d finite cells. Therefore we discretise Ω by a union of finite cells ω_j

$$\Omega = \cup_{j=1}\omega_j,\ \omega_j \cap \omega_i = N,\ \text{measure of } N \text{ equals zero.}$$

For example by balancing the equations (4) over ω_j we get a system of K equations of type

$$\mathbf{U}_j^n - \frac{\tau}{\mu}\Delta_h\mathbf{U}_j^n = \beta(\mathbf{Z}_j^{n-1}) + \frac{\tau}{\mu}f(\mathbf{Z}_j^{n-1}) \quad j = 1,\dots,K,$$
$$\mathbf{Z}_j^n := \mathbf{Z}_j^{n-1} + \mu(\mathbf{U}_j^n - \beta(\mathbf{Z}_j^{n-1})) \quad j = 1,\dots,K, \tag{5}$$

where we closed the system by including the boundary conditions.

Δ_h is a finite approximation of the Laplacian Δ. In the finite volume discretisation method the discretisation of a diffusion term Δu is done as follows. We start with the integral balance

$$\int_\Omega \Delta u \, dv$$

and

$$\int_\Omega \Delta u \, dv = \sum_{j=1}^{K} \int_{\omega_j} \Delta u \, dv$$

is obvious. Now we use the theorem of Gauß-Ostrogradski (divergence-theorem) to move to flux integrals

$$\int_{\omega_j} \Delta u \, dv = \sum_{s=1}^{j_s} \int_{\gamma_{js}} \nabla u \cdot \mathbf{n}_{\gamma_{js}} \, d\partial\gamma_{js} \tag{6}$$

where j_s is the number of boundary pieces γ_{js} of the finite-volume/cell ω_j. The fluxes or directional derivatives $\nabla u \cdot \mathbf{n}_{\gamma_{js}}$ are now approximated by finite differences of values of the u-values in the cell-centers. In the case of simple structured grids the cells are rectangles and the number of boundary parts of all cells are equal to 4. The sum of the right side of (6) together with the approximated fluxes is the finite approximation of Δu.

For the Euler-backward time integration method we get, starting from (3)

$$\frac{\mathbf{Z}_j^n - \mathbf{Z}_j^{n-1}}{\tau} = \Delta_h \beta(\mathbf{Z}_j^n) + f(\mathbf{Z}_j^n) \quad j = 1, \cdots, K, \tag{7}$$

(also by closing the system by using the boundary information). The term $\Delta_h \beta(\mathbf{Z}_j^n)$ is more complicated as the corresponding term $\Delta_u \mathbf{U}_j^n$.

We have to mention that in the 1d case or in the case of structured equidistant grids in 2d problems the finite-volume method is very close to finite-difference methods.

5 Solution Methods for the Linear Equations (5) and the Non-linear Systems (7)

The linear systems (5) are solved by iterative Krylov-space methods or by direct methods (Gauß). For the nonlinear systems (7) we use the Trust-Region-Dogleg-, the Trust-Region- and the Levenberg-Marquard-Algorithm. We took these algorithms given by Matlab or Octave. The non-linear algorithms are realised by the fsolve-command und the linear solution one get by the backslash-command.

But during our numerical experiments we observed, that the ressources of Matlab or Octave are not good enough to solve problems with very fine spatial discretisations.

6 Numerical Experiments - 1d

The following 1d- and 2d-examples are part of the master-thesis [5], where one can find a lot of other instructive numerical examples.

First we considered a 1d examples with 2 species ($M = 2$). To recognise the functions β and f we state the relevant equation system

$$\begin{aligned}\frac{\partial z_1}{\partial t} &= \Delta[(a_1 + b_1 z_1 + c_1 z_2)z_1] + (g_{10} - g_{11}z_1 - g_{12}z_2)z_1,\\ \frac{\partial z_2}{\partial t} &= \Delta[(a_2 + b_2 z_2 + c_2 z_1)z_2] + (g_{20} - g_{21}z_1 - g_{12}z_2)z_2,\end{aligned}$$

Based on this system we define 3 test-examples. The first one reads as

$$\begin{aligned}\frac{\partial z_1}{\partial t} &= \Delta[(0,04 + 0,04\alpha z_2)z_1] + (2,8 - 1,1z_1 - z_2)z_1,\\ \frac{\partial z_2}{\partial t} &= \Delta[(0,04 + 2\alpha z_1)z_2] + (3,0 - z_1 - 1,1z_2)z_2,\end{aligned} \tag{8}$$

We work with $\alpha = 1$. For $\alpha = 0$ the initial value $(z_1, z_2) = (\frac{8}{21}, \frac{50}{21})$ gives a stable steady state solution. Therefore we use the initial value

$$\begin{aligned}z_1(x,0) &= \frac{8}{11} + \frac{8}{11}R/100\\ z_2(x,0) &= \frac{50}{11} + \frac{50}{11}R/100\end{aligned}$$

where $R \in \mathbb{R}$ is an equally distributed random number of the interval $(0, 1)$. As Ω we use in this 1d example the unit interval. For all species we use homogeneous Neumann boundary conditions.

Space grid size h	$\tau = 2^{-5}$ (linear)	$\tau = 2^{-5}$ (nonlinear)	$\tau = 2^{-7}$ (linear)	$\tau = 2^{-7}$ (nonlinear)
1/8	0,14	7,57	4,28	21,15
1/16	0,25	11,77	8,00	36,44
1/32	0,49	16,48	15,44	66,37
1/64	0,95	63,27	30,47	249,51
1/128	1,90	241,09	60,61	958,09
1/265	3,83	970,58	121,92	3913,63

This table shows the computational times to reach a steady state solution (on a quad core personal computer, the times can be proportional scaled to computers with higher performance). For the solution with the linear algorithm we got a linear growth of the times with respect to the used grid refinement. On the other hand the growth of the computational times of the nonlinear algorithm is

exponential. The influence of μ in this example was not significant. We used for all species $\mu = 1$.

As a second 1d example we consider the cross-diffusion system

$$\begin{aligned}\frac{\partial z_1}{\partial t} &= \Delta[(10^{-5} + 10^{-2}z_1 + 10^{-1}z_2)z_1] + (2,8 - 1,1z_1 - z_2)z_1,\\ \frac{\partial z_2}{\partial t} &= \Delta[(10^{-5} + 10^{2}z_1 + 10^{-2}z_2)z_2] + (3,0 - z_1 - 1,1z_2)z_2,\end{aligned} \tag{9}$$

As initial conditions we use

$$\begin{aligned}z_1(x,0) &= \frac{8}{11}(1 - 0,1\exp(-x^2))\\ z_2(x,0) &= \frac{50}{11}(1 + 0,1\exp(-x^2))\end{aligned}$$

for $x \in (0,1)$. Homogeneous Neumann boundary conditions are used. For the first species we use $\mu = 7$ and or the second one $\mu = 0.03$.

The computational times for the solution of the second 1d example are similar to those of the first example.

As a third 1d example we consider the equation system

$$\begin{aligned}\frac{\partial z_i}{\partial t} &= \Delta\beta_i(\mathbf{z}) + d_i\mathrm{div}(z_i\nabla p) \quad \text{in} \quad \Omega\\ \frac{\partial\beta_i(\mathbf{z})}{\partial\nu} &+ d_i z_i\frac{\partial p}{\partial\nu} = 0 \quad \text{on} \quad \partial\Omega\times(0,T),\\ z_i(\cdot,0) &= z_{0i} \quad \text{in} \quad \Omega\end{aligned} \tag{10}$$

with $\beta_i(\mathbf{z}) = (a_i + b_i z_i + c_i z_j)z_i$ for $(i,j) \in \{(1,2),(2,1)\}$, $p(x) = 1.5(x - 0.5)^2$, $z_{10} = 10$, $z_{20} = 20$. In this example we use $\Omega =]0, L[=]0,3[$ and $]0,T] =]0,10]$.

As a discretisation of the system (10) we use the finite difference or finite volume method resp. The coefficients $a_i = c_i = d_i = 1$ are fixed. For the coefficients b_i we use the values 0 and 0.1. The spatial discretisation parameter is $h = L/N_X$ where $N_X + 1 = 301$ is the number of mesh points. The time-step parameter is $\tau = 10^{-3}$ and $N_T = T/\tau$ is the number of time-levels. For μ we used the value 10^{-3}.

Let $Z_i^{j,n}$ be the numerical approximation of $z_i(jh, n\tau)$. For the numerical solution $\{Z_i^{j,n-1}\}_{i=1,2,j=0,\ldots,N}$, $(n = 1,\ldots,N_T)$, is to solve

$$\begin{aligned}U_i^{j,n} - \frac{\tau}{\mu h^2}(U_i^{j+1,n} - 2U_i^{j,n} + U_i^{j-1,n})\\ -\frac{d_i\tau}{2h}(U_i^{j+1,n} - U_i^{j-1,n})p_x(jh) - d_i\tau U_i^{j,n}p_{xx}(jh)\\ = \beta_i(\mathbf{Z}^{j,n-1}) + \frac{d_i\tau}{2\mu h}(\mathbf{Z}^{j+1,n-1} - \mathbf{Z}^{j-1,n-1} - \mu\beta_i(\mathbf{Z}^{j-1,n-1}))p_x(jh)\\ +\frac{d_i\tau}{\mu}(\mathbf{Z}^{j,n-1} - \mu\beta_i(\mathbf{Z}^{j,n-1}))p_{xx}(jh),\\ \frac{U_i^{-1,n} - U_i^{1,n}}{2h} - d_i(\mathbf{Z}^{0,n-1} - \mu(U_i^{0,n} - \beta_i(\mathbf{Z}^{0,n-1})))p_x(0) = 0,\end{aligned}$$

$$\frac{U_i^{N_X+1,n} - U_i^{N_X-1,n}}{2h} + d_i(\mathbf{Z}^{N_X,n-1} - \mu(U_i^{N_X,n} - \beta_i(\mathbf{Z}^{N_X,n-1})))p_x(L) = 0,$$

to get with $\{U_i^{j,n}\}_{i=1,\ldots,M,\, j=0,\ldots,N_X}$ the U-values at the new time-level n. After that we compute with

$$Z_i^{j,n} = Z_i^{j,n-1} + \mu(U_i^{j,n} + \beta_i(\mathbf{Z}^{j,n-1})$$

the values $\{Z_i^{j,n}\}_{i=1,2,\, j=-1,\ldots,N_X+1}$ at the new time-level.

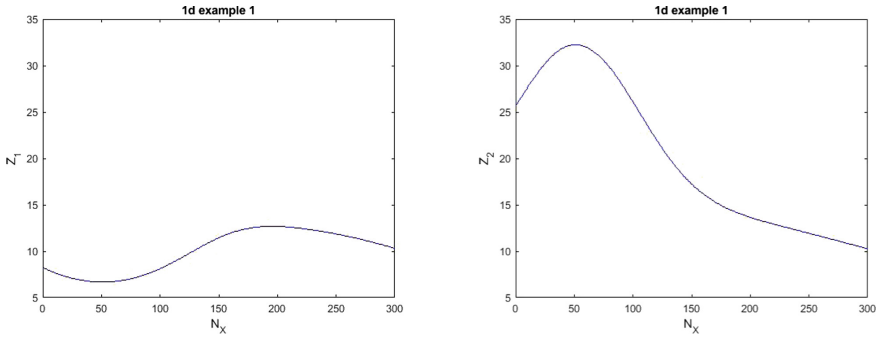

Fig. 1. 1d solution, 3rd example, first (left) and second (right) species, with $b_i = 0$

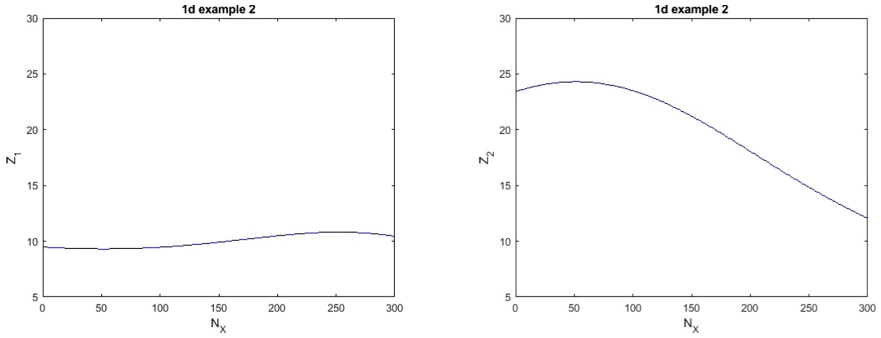

Fig. 2. 1d solution, 3rd example, first (left) and second (right) species, with $b_i = 0, 1$

The results showed in Figs. 1 and 2 represent the steady states. The computations were finished when the condition

$$\max_{0<j<N_X} \frac{|Z^{j,n} - Z^{j,n-1}|}{|Z^{j,n-1}|} < 10^{-5} \tag{11}$$

was fulfilled.

In the 4th example we considered the same model (9) as in the 3rd one. We consider large diffusion coefficients a_i compared to b_i. The coefficients $b_i = 0,001$, $c_i = d_i = 1$ are fixed. The Figs. 3 and 4 show the results for $a_i = 10$ and $a_i = 100$.

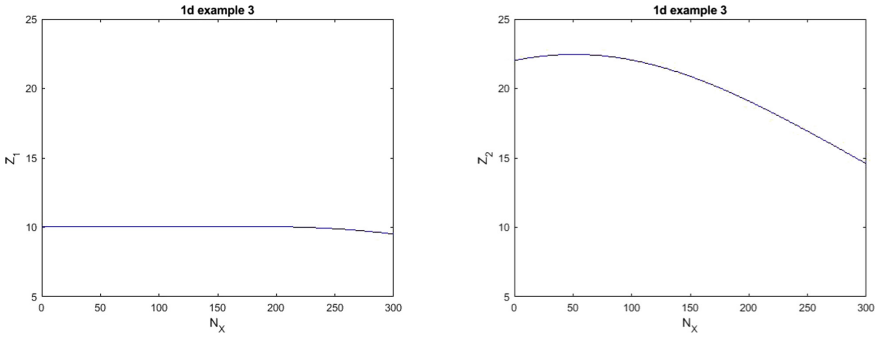

Fig. 3. 1d solution, 4th example, first (left) and second (right) species, with $a_i = 10$

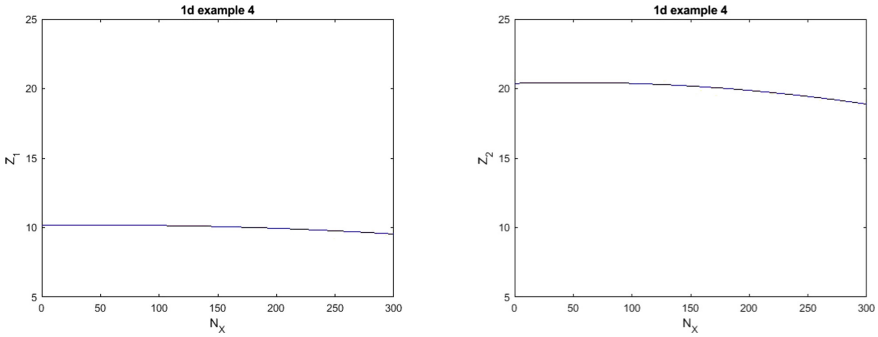

Fig. 4. 1d solution, 3rd example, first (left) and second (right) species, with $a_i = 100$

The steady states are reached if the condition (11) was fulfilled.

7 Numerical Experiments - 2d

For the 2d experiments we consider

$$\begin{aligned} \frac{\partial z_1}{\partial t} &= \Delta[(0,04 + 0,04z_2)z_1] + (2,8 - 1,1z_1 - z_2)z_1, \\ \frac{\partial z_2}{\partial t} &= \Delta[(0,04 + 2z_1)z_2] + (3,0 - z_1 - 1,1z_2)z_2, \end{aligned} \tag{12}$$

on $\Omega = (0,1)^2$. As initial conditions we use

$$\begin{aligned} z_1(x,y,0) &= \frac{8}{11} + \frac{8}{11}R/100 \\ z_2(x,y,0) &= \frac{50}{11} + \frac{50}{11}R/100 \end{aligned}$$

with the above described random number R.

In the following table we compare the computational times of the linear and nonlinear methods for the 2d example. We used an equidistant discretisation.

Grid size $h_x = h_y$	Linear algorithm	Nonlinear algorithm
1/4	0,03	0,63
1/8	0,14	8,57
1/16	0,45	151,99
1/32	1,80	1850,22
1/64	7,45	29405,92

As a second 2d example we consider the cross diffusion system

$$\begin{aligned} \frac{\partial z_1}{\partial t} &= \Delta[(10^{-5} + 10^{-2}z_1 + 10^{-1}z_2)z_1] + (2,8 - 1,1z_1 - z_2)z_1, \\ \frac{\partial z_2}{\partial t} &= \Delta[(10^{-5} + 10^{2}z_1 + 10^{-2}z_2)z_2] + (3,0 - z_1 - 1,1z_2)z_2, \end{aligned} \tag{13}$$

with the initial conditions

$$\begin{aligned} z_1(x,y,0) &= \frac{8}{11}(1 - 0,1\exp(-(x^2+y^2))) \\ z_2(x,y,0) &= \frac{50}{11}(1 + 0,1\exp(-(x^2+y^2))). \end{aligned}$$

We follow the solution in the time during $S = [\frac{3}{\tau}]$[1] time steps. We use an equidistant discretisation $h_x = h_y = \frac{1}{64}$ and $\tau = 2^{-6}$. The solution of this problem faults with the use of the μ-values of the second 1d example ($\mu_1 = 7$ for the first species and $\mu_2 = 0,03$ for the second one).

Here we investigate the behaviour of the nonlinear method for different values of μ_1, namely $\mu_1 \in \{0,03,\ 0,5,\ 1,\ 2,5\}$.

The following Figs. 5, 6, 7 and 8 show that there will be a influence of μ to the time position of the solution. The figures show that small values of μ show results, which are closer to the wanted steady state.

[1] The function $[q]$ gives the largest integer back, which is less than q.

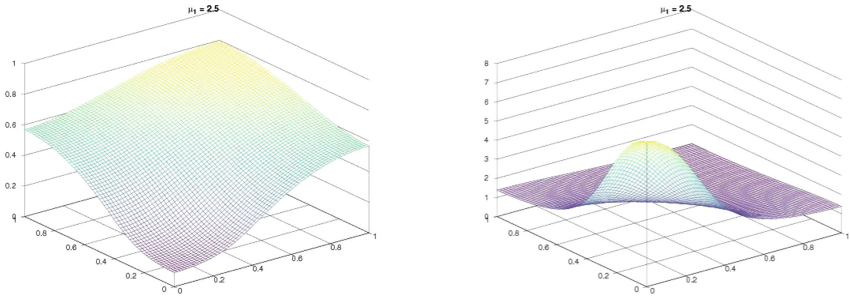

Fig. 5. 2d solution, first and second species, with $\mu = 2,5$

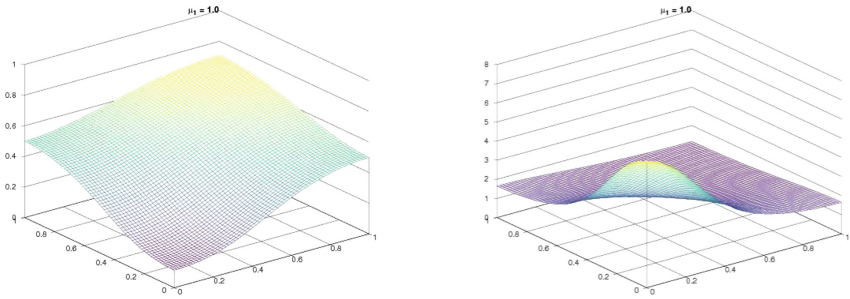

Fig. 6. 2d solution, first and second species, with $\mu = 1,0$

8 Resumee

First of all we have to note, that it is very useful to have linear time-integration schemes to approximate cross-diffusion systems. Thus we can save a lot of computational time compared to nonlinear systems coming from implicit Euler-backward discretisation. Especially the growth of the computational time with respect to the spatial grid refinement of the linear scheme is significantly slower then the time growth of the nonlinear scheme.

The analysis of the test examples in which occur convergence and stability problems during the numerical solution shows that this is the case if we have a very strong cross-diffusion, which results in weakening the parabolicity of the system.

The choice of the parameter μ is also a crucial point with respect to time-truth of the numerical solution. The choice of appropriate time and space discretisation parameters, τ and h, must be further investigated. Especially the space grid resolution must be fine enough to resolve fine-scale properties of the solution in case of complicated initial distributions of the species.

If we are only interested in steady state solutions the choice of μ has no influence. Certain choices of different μ values falsify the time of the modeled process on the other hand, i.e. for different values of μ the solutions after a

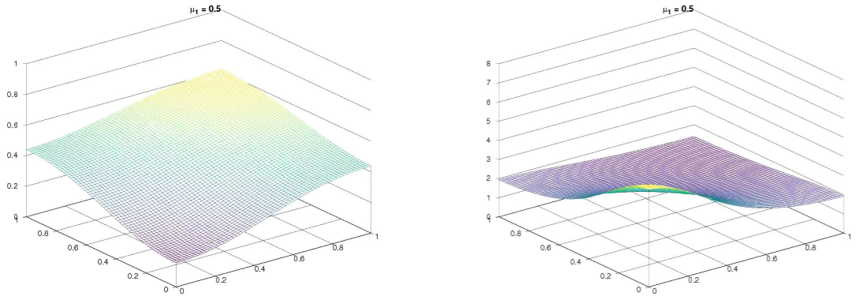

Fig. 7. 2d solution, first and second species, with $\mu = 0,5$

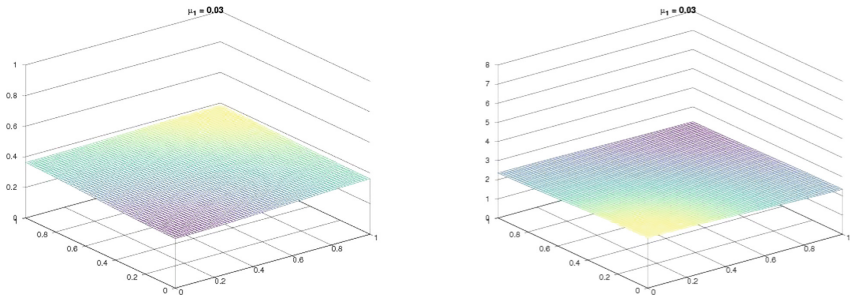

Fig. 8. 2d solution, first and second species, with $\mu = 0,03$

certain time-step n (that is $t = n\tau$) differ. The use of different μ values faster the modeled process or slowed down the process.

At the end our experiences with linear time discretisation scheme are very promising. But there must still investigate applicable rules for the choice of the time and space discretisation parameters and the choice of the free parameter μ.

References

1. Shigesada, N., Kawasaki, K., Teramoto, E.: Spatial segregation of interacting species. J. Theor. Biol. **79**, 83–99 (1979)
2. Murakawa, H.: A linear scheme to approximate nonlinear cross-diffusion systems. ESAIM: M"AN **45**, 1141–1161 (2011)
3. Murakawa, H.: Error estimates for discrete-time approximation of nonlinear cross-diffusion systems. SIAM J. Numer. Anal. **52**(2), 955–974 (2014)
4. Chen, L., Jüngel, A.: Analysis of a multidimensional parabolic population model with strong cross-diffusion. SIAM J. Math. Anal. **36**, 301–322 (2006)
5. Baumbach, J.: Numerische Untersuchungen eines linearen Zeitintegrationsschemas für nichtlineare Kreuz-Diffusionsprobleme. Master-thesis, TU Berlin (2018)